STRESS-DENSITY VARIATIONS IN ALUMINA SEDIMENTS: EFFECTS OF POLYMER CHEMISTRY

C. H. SCHILLING,* J. J. LANNUTTI,# W.-H. SHIH,# and I. A. AKSAY#

*Pacific Northwest Laboratory,+ Richland, WA 99352
#Department of Materials Science and Engineering; and
Advanced Materials Technology Center, Washington Technology Center,
University of Washington, Seattle, WA 98195

INTRODUCTION

Achieving spatially uniform and hierarchically structured microstructures during the shape-forming of colloidal ceramics depends largely on (*i*) the magnitude of the effective stresses (i.e., stresses that are supported by the particulate network) and (*ii*) plastic properties, which in turn are significantly altered by processing parameters affecting interparticle friction and adhesion. To quantify the effects of processing parameters on consolidation, we present a novel approach for analyzing sediments by gamma-ray densitometry[1] and a fluid mechanics model. This method enables us to correlate processing parameters with spatial variations of the packing density and the local effective stress. These correlations are difficult to achieve by traditional techniques (e.g., rheometry, sedimentation kinetics modeling, soil mechanics tests), especially for the low stresses (< 1000 Pa) that are typically encountered in sediments. Aside from being destructive to samples, these techniques also tend to measure volume-averaged properties, and as a result they usually fall short of describing localized consolidation phenomena.

Significant variations in plasticity can arise through modification of interparticle forces by changing the chemistry of surface-adsorbed polymers or ions. In the present study, we address the question of how to design surface-adsorbed polysiloxanes to enhance particle rearrangement into densely packed structures. Polysiloxanes are excellent lubricants (e.g., silicon oil) due to the low rotational energy of the Si–O–Si bonds comprising the polymer backbone. These inorganic polymers are also available with a broad range of chemical structures that can pyrolyze to various inorganic silicon-based compounds under appropriate conditions.[2] This research is part of a larger program examining the use of polymeric additives that may form useful inorganic phases within the pores of a ceramic compact upon pyrolysis.[3]

We analyzed stress-density correlations of alumina sediments as a function of two major variations in additive chemistry: (*i*) the attachment of polar (carbonyl) pendants to the siloxane backbone, and (*ii*) changes in the molecular weight of nonpolar $[MeHSiO]_x$ (hydrosiloxane). We suspect that the carbonyls may enhance particle rearrangement since these moieties are the primary constituents of organic polymers (e.g., polymethacrylic acid) which are used to increase packing density.[4] A sample containing fluorinated polyester, an organic polymer which has previously been shown to promote the formation of high green densities in alumina cakes,[5] was also analyzed for comparison with the inorganic polymers. In addition, we analyzed a sample prepared with an aluminosiloxane polymer that pyrolizes to mullite ($3Al_2O_3{\cdot}2SiO_2$).[2]

+ Pacific Northwest Laboratory is operated for the U.S. Department of Energy by Battelle Memorial Institute under Contract DE-AC06-76RLO 1830.

EXPERIMENTAL PROCEDURE

Five starting solutions were prepared using dry chloroform and one of the following polymers: fluorinated polyester (FPE), polyacryloxypropylsiloxane (PAS), a mullite-forming aluminosiloxane (MF), and hydrosiloxanes of two different molecular weights.** Figure 1 shows the chemical structures of the polymers. Each of the hydrosiloxane solutions contained polymers with either four (HS4) or approximately twenty-two (HS22) monomers per chain. Each solution contained approximately 4 x 10^{18} polymer molecules per ml. Four vol% α-Al_2O_3 particles*** was added to each solution, which was followed by 10 minutes of ultrasonication. Of each suspension, 180 ml were subsequently poured into Pyrex sedimentation tubes (3 cm inside diameter). Each tube was pre-treated with $(CH_3)_3SiCl$ solution to reduce shear stresses at the inner wall.[2,3]

During sedimentation, local measurements of packing density were obtained by gamma-ray densitometry.[1] Each sediment was irradiated by a 3.2-mm-diameter collimated beam of photons (661 keV) emitted from cesium-137. Photon transmission was measured at each elevation, z, and related to the volume fraction of solids, ϕ, (accuracy $\pm$ 0.015) using the Beer-Lambert law. We assume that ϕ is uniform within the irradiated volume at each elevation.

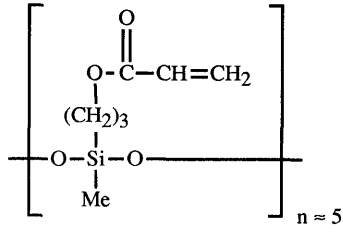

Figure 1a. Polyacryloxypropylsiloxane (PAS).

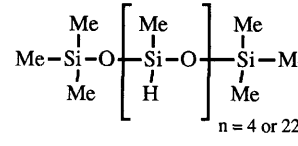

Figure 1b. Hydrosiloxane.

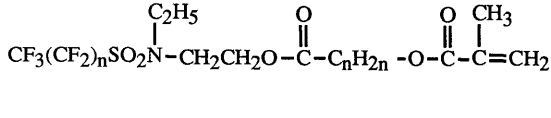

Figure 1c. Fluorinated polyester (FPE); molecular weight ≈ 800.

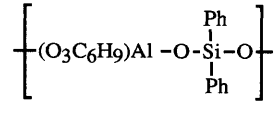

Figure 1d. "Mullite-former" (MF); molecular weight ≈ 800.

RESULTS AND DISCUSSION

All suspensions appeared to be flocculated, based on the rapid initial settling rates (≈ 1 cm/min) and the visibly transparent supernatants that remained above each sediment throughout the experiment. At the conclusion of visible sedimentation, the density profiles remain time-invariant, as shown in Figure 2. The hydrosiloxane samples exhibited nonuniform packing and relatively low solids fractions ($0.16 < \phi < 0.38$) that increased with decreasing elevation, although HS4 had slightly greater densities.

** FPE was obtained from 3M Corporation, Minneapolis, Minn. The remaining polymers were obtained from Huls Petrarch Systems, Bristol, Penn.

*** 0.4 μm average diameter, Type AKP-30, Sumitomo Chemical America, New York, N.Y.

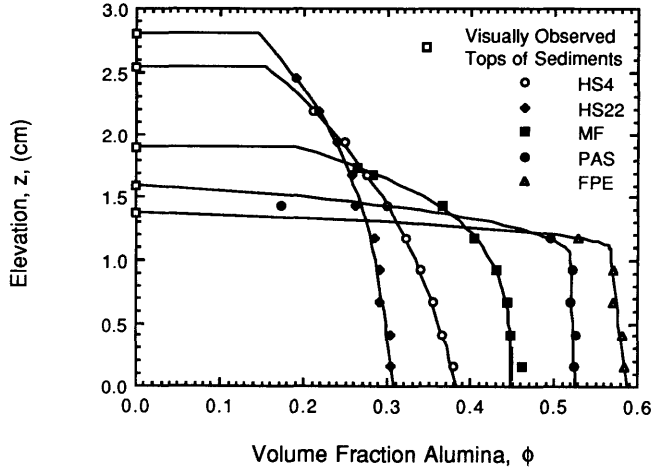

Figure 2. Density profiles for the equilibrium sediments as a function of polymer chemistry.

The MF sample appeared to consist of a densely packed lower layer ($\phi \approx 0.45$) of approximately 1 cm in thickness and an upper layer having lower densities and approximately the same thickness. The FPE and PAS samples exhibited greater maximum densities of 0.58 and 0.53, respectively.

As shown in Figure 2, we curve fitted the density functions by setting the integrated area under each curve approximately equal to the known true volume of powder (7.2 cm^3) in each sample:

HS4: $\phi = -6.23544(10^{-3})z^3 - 4.08715(10^{-3})z^2 - 4.000812(10^{-2})z + 0.3847906$; $(0 \le z \le 2.54$ cm); (1)

HS22: $\phi = -6.55993(10^{-3})z^3 + 5.09235(10^{-3})z^2 - 2.147357(10^{-2})z + 0.3092194$; $(0 \le z \le 2.79$ cm); (2)

PAS: $\phi = -5.590529(10^{-3})z + 0.5265175$; $(0 \le z^* \le 1.0$ cm); (3)

$\phi = -5.5200292(10^{-1})z^4 + 1.18777395z^3 - 7.8881246(10^{-1})z^2 + 1.5629941(10^{-1})z + 0.5226283$; $(1.0 < z \le 1.6$ cm); (4)

FPE: $\phi = -1.854329(10^{-2})z + 5.878838(10^{-1})$; $(0 \le z \le 1.105$ cm) (5)

$\phi = -3.31288603z^6 + 10.2322178z^5 - 11.65428686z^4 + 6.02684442z^3 - 1.41215531z^2 + 1.12755(10^{-1})z + 0.5846$; $(1.105 < z \le 1.37$ cm); (6)

MF: $\phi = -2.4279(10^{-2})z^4 + 2.1792(10^{-2})z^3 - 3.0148(10^{-2})z^2 + 8.1956(10^{-3})z + 0.44995$; $(0 \le z \le 1.905$ cm). (7)

It was not possible to resolve the exact shapes of the density profiles within the uppermost regions of each sample because of the relatively large diameter of the photon beam. However, based on the experimental curve fits above, we can infer that the PAS and FPE samples consisted of two layers: a thick, lower layer of uniform high density, and a thin, upper layer of lower densities. As further evidence, we also analyzed a set of curve fits that assumed the absence of a two-layer structure in the PAS and FPE samples; in each case ϕ was expressed as a linear function of z at all elevations, and the integrated areas significantly exceeded the known mass of powder in each sample. It should be mentioned that more accurate density profiles are possible by collimating the beam to a smaller size.

Equations (1) through (7) were used to calculate spatial variations of the effective stress using a fluid statics model.[6-8] The model assumes that, during settling, flocculated particle networks form an elastic continuum that transmits the weight, buoyancy, and viscous drag forces from one elevation to the next. Shear stresses acting from the walls of the sedimentation tubes are also neglected. The net force transmitted by the network at a particular elevation is simply equal to the dynamic balance of the above forces summed over the entire network above that elevation. For stable cakes, the viscous drag component is zero:

$$P(z^*) = \int_{z^*}^{z_{max}} \Delta\rho \; g \; \phi \; dz \qquad (8)$$

where $P(z^*)$ is the effective stress at an elevation of z^*, z_{max} is the sediment height, $\Delta\rho = 2.47$ g/cm^3 is the density difference between the solid and liquid, and g is the gravity acceleration constant. After substituting equations (1) through (7) into (8), we plotted $P(z^*)$ as a function of the local density at z^* (Figure 3). Results indicate that ϕ plots as a series of approximately linear functions of ln $P(z^*)$, a trend that was previously reported for alumina cakes by measuring volume-averaged densities during drained uniaxial compression.[9,10] Similar behavior was also reported for flocculated sediments of thoria[7] (ThO_2) and microbarite[8] ($BaSO_4$).

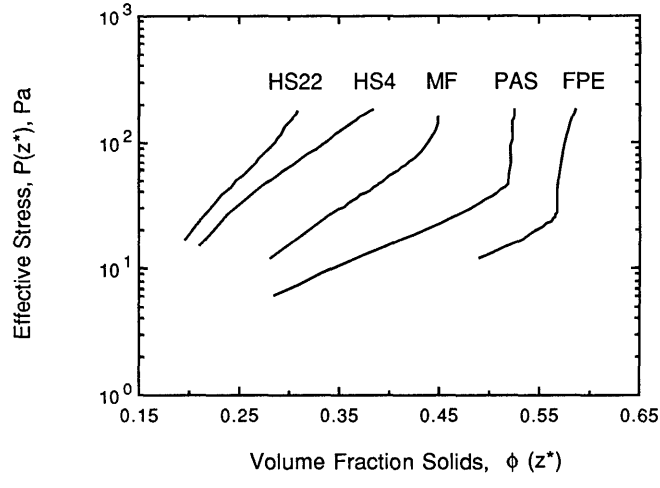

Figure 3. Effective stress as a function of packing density and polymer chemistry.

The slope and position of a given ϕ – ln P(z*) plot reveal important information regarding the effects of suspension chemistry on particle rearrangement. The slope, $d[\ln P(z^*)]/d\phi$, can be interpreted as an activation barrier for rearrangement, α, based on a model reported by Shih et al.[10,11] This model proposes that a change in density, $d\phi$, due to an increment in effective stress, dP(z*), is proportional to the probability of overcoming an energetic barrier whose height is proportional to the local density. Thus, $d\phi/dP(z^*) = \exp[-\alpha\phi]$. Integrating and rearranging, one obtains $P \approx \exp(\alpha\phi)$, as indicated in Figure 3. The activation barrier can be affected by changes in processing parameters that influence interparticle attraction.

A striking feature of Figure 3 is that α for the MF, PAS, and FPE samples abruptly increases at a critical point that is uniquely characteristic of the polymer chemistry. These abrupt increases in α correspond to the approximate elevations of the interfaces between the low- and high-density layers in these samples. Also, when successively comparing MF to PAS to FPE, we observe that (*i*) the critical density increases, (*ii*) the thickness of the low-density layer decreases, and (*iii*) below the critical densities, α decreases from approximately 20 to 10. We believe that these trends may be attributed to a reduction in interparticle attraction, although additional experiments with well-defined attractive interparticle potentials are needed to confirm this hypothesis.

The presence of a two-layer structure is not suggested by the density profiles of the hydrosiloxane samples; as a result, these samples exhibit α values ($\approx$ 20) that were approximately independent of z, ϕ, and P(z*). A decrease in the hydrosiloxane molecular weight, however, decreases the α value and hence increases the local density at a particular effective stress. It is possible that the hydrosiloxane samples may exhibit an abrupt increase in α by increasing the effective stress, e.g., by increasing the alumina concentration of the starting suspension or by using taller sedimentation columns.

We learned that slight differences in curve fitting the density functions will not influence the general shapes of the plots in Figure 3, but they may change the values of α and the exact locations of the critical points. For example, the above calculations were repeated by varying the curve fit within the low-density layer of the PAS sample, and we observed small effects on both the critical density and α values for densities below the critical density. The critical effective stress, however, varied by as much as 10 Pa. We also learned that slight variations in the curve fit for densities above the critical density may produce large uncertainties in α above the critical density. As a result, we cannot specify reliable α values for densities above the critical density because of experimental measurement uncertainty.

Additional studies are needed to further investigate the presence of layered microstructures in sediments and to establish correlations between α, interparticle attraction-repulsion forces, and microscopic mechanisms of particle network restructuring in these layers. Direct imaging, e.g., by high-resolution computerized tomography or electron microscopy, would be beneficial to quantify spatial variations of structural features, especially those that may be responsible for the existence of layered structures in sediments. In addition, useful information can be obtained by the use of theoretical models that relate macroscopic properties, such as stress and packing density, to interparticle attraction/repulsion energies and microstructural deformation processes.[11-15]

CONCLUSIONS

A novel analytical technique is presented, which uses densitometry and fluid mechanics modeling to correlate spatial variations of the packing density and local effective stress in sediments. Using this technique, we show that the consolidation behavior of chloroform-alumina sediments is significantly affected by the chemistry of polysiloxane additives. Nonpolar hydrosiloxanes resulted in relatively poor packing behavior with a smooth gradient in density from the bottom to the top of each sample. The activation barriers in these samples remained at high values that were independent of elevation and density for solids fractions of up to 0.38. Slight improvements in packing were obtained by decreasing

the hydrosiloxane molecular weight. In contrast, samples containing polyacryloxypropylsiloxane, fluorinated polyester, and a mullite-forming aluminosiloxane exhibited "two-layer" microstructures consisting of (*i*) a densely packed bottom layer and (*ii*) a top layer having lower densities. At the interfaces between these two layers, the activation barriers exhibited an abrupt transition from low values, occurring within the top layers, to high values occurring in the bottom layers. Variations in the thickness of each layer and the critical densities associated with the activation barrier transitions were uniquely characteristic of the polymer chemistry and may be attributed to changes in interparticle attraction.

ACKNOWLEDGMENTS

This work was supported by the Office of Basic Energy Sciences, U.S. Department of Energy, through a subcontract by Pacific Northwest Laboratory under Contract No. 063961-A-F1. The authors wish to thank Dr. Wan Shih for valuable discussions.

REFERENCES

1. C. H. Schilling, G. L. Graff, W. D. Samuels, and I. A. Aksay, in ***Atomic and Molecular Processing of Electronic and Ceramic Materials: Preparation, Characterization, and Properties, MRS Conf. Proc.***, edited by I. A. Aksay, G. L. McVay, T. G. Stoebe, and J. F. Wager (Materials Research Society, Pittsburgh, Pennsylvania, 1988), p. 239.
2. J. J. Lannutti, Ph.D. Thesis, University of Washington, 1990.
3. J. J. Lannutti, C. H. Schilling, and I. A. Aksay, in ***Processing Science of Advanced Ceramics, MRS Symp. Proc.***, Vol. 155, edited by I. A. Aksay, G. L. McVay, and D. R. Ulrich (Materials Research Society, Pittsburgh, Pennsylvania, 1989), p. 155.
4. J. Cesarano III, I. A. Aksay, and A. Bleir, *J. Am. Ceram. Soc.*, **71**, 240 (1988).
5. D. Gallagher, Ph.D. Thesis, University of Washington, 1988.
6. R. Buscall, *Colloids and Surfaces*, **5**, 269 (1982).
7. H. A. Kearsey and L. E. Gill, *Trans. Inst. Chem. Engrs.*, **41**, 296 (1963).
8. F. M. Tiller and Z. Khatib, *J. Colloid Interface Sci.*, **100**, 55 (1984).
9. F. F. Lange and K. T. Miller, *Bull. Am. Ceram. Soc.*, **66**, 1498 (1987).
10. W.-H. Shih, S. I. Kim, W. Y. Shih, C. H. Schilling, and I. A. Aksay, in ***Better Ceramics Through Chemistry IV, MRS Symp. Proc.***, Vol. 180, edited by C. H. Brinker, D. E. Clark, D. R. Ulrich, and B. J. J. Zelinski (Materials Research Society, Pittsburgh, Pennsylvania, 1990), p. 167.
11. W. Y. Shih, W.-H. Shih, and I. A. Aksay, in ***Physical Phenomena in Granular Materials***, Vol. 195, edited by G. D. Cody, T. H. Geballe, and P. Sheng (Materials Research Society, Pittsburgh, Pennsylvania, 1990), p. 477.
12. W. Y. Shih, I. A. Aksay, and R. Kikuchi, *Phys. Rev. A*, **36**, 5015 (1987).
13. W.-H. Shih, W. Y. Shih, S. I. Kim, J. Liu, and I. A. Aksay, *Phys. Rev. A*, **42**, 4772 (1990).
14. L. T. Kuhn, R. M. McMeeking, and F. F. Lange, in ***Powders and Grains***, edited by J. Biarez and R. Gourves (Balkema, Rotterdam, 1989), p. 331.
15. P. A. Cundall, J. T. Jenkins, and I. Ishibashi, in ***Powders and Grains***, edited by J. Biarez and R. Gourves (Balkema, Rotterdam, 1989), p. 319.